Experimental study of reflooding heat transfer on Cr-layered cladding under atmospheric pressure

Doyoung Shin [a], Namgook Kim [a], Sung Joong Kim [a,b*]

[a]Department of nuclear engineering, Hanyang University, 222 Wangsimni-ro, Seongdong-gu, Seoul 04763, Republic of Korea

[b]Institute of nano science and technology, Hanyang University, 222 Wangsimni-ro, Seongdong-gu, Seoul 04763, Republic of Korea

[*]Corresponding author: sungjkim@hanyang.ac.kr

1. Introduction

Many research and development (R&D) programs have been launched after Fukushima nuclear disaster to develop accident-tolerant fuel (ATF) to mitigate oxidation of cladding materials [1]. Among many candidates, the surface modification of existing Zr based cladding by means of coating a thin layer with strong oxidation resistant materials (e.g. Cr, FeCrAl, SiC, etc.) showed promising performance with affordable cost.

However, once the heat transfer surface is modified, it exhibits different or sometimes unexpected boiling heat transfer characteristics and may alter the thermal safety margin [2]. Thus in order to ensure the safety of nuclear power plant, the performance of the ATF cladding should be evaluated under meaningful thermal-hydraulic conditions such as core reflooding condition accompanied by the safety injection during loss-of-coolant-accident (LOCA).

Recently, many studies have investigated the quench performance of ATF materials [3-5]. However, these studies lack of important characteristics which are expected to appear during the reflood of the core. Firstly, because the previous studies utilized a furnace to externally heat up the specimens, the decay heat effect could not be considered. Secondly, flow effect was neglected because the heated specimen was simply immersed into the water pool at high speed. Thus in addition to the modified surface effect, aforementioned issues need to be addressed for the performance of ATF cladding during the reflood phase.

So the objective of this study is to investigate the reflood heat transfer performance of Cr-coated Zr-alloy cladding. We designed internally heated specimen capable of simulating the decay heat and slowly injected the water to investigate the flow effect. Comparison of critical heat flux (CHF), minimum film boiling temperature (MFBT), and high-speed visualization images between the bare and Cr-coated surfaces was carried out.

2. Experiment setup

2.1 Experimental apparatus and test specimen

The experimental apparatus used in this study is shown in Fig. 1. The test specimen was Zr-based alloy tube with 9.53 mm in diameter and 100 mm in length. The specimen was heated by Joule heating of Inconel 600 rodlet with diameter of 5 mm installed inside. ZrO_2 ceramic pellet was inserted in the gap to conduct heat to the surface. The test specimen was electrically isolated from the copper electrodes to prevent any heat generation in the cladding. Two thermocouples (TCs) with sheath diameter of 0.5 mm were installed at the grooved lines in ZrO_2 right below the cladding surface at two axial locations (i.e. z=20 and 60 mm).
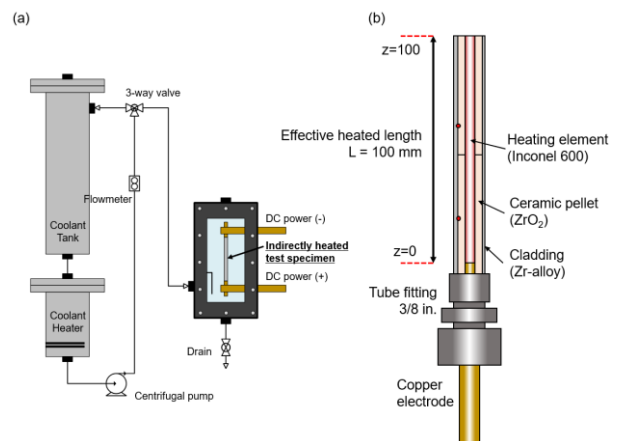
Fig. 1. Schematics of (a) Experimental apparatus and (b) test specimen design. Red dots indicate the location of TCs.

2.2 Surface preparation

Before depositing the Cr-layer, the cladding surfaces were initially ground by sandpaper of grit number of 320 to reserve the same intrinsic surface roughness. The micro-scratches were formed in circumferential direction. The Cr coating was carried out by means of DC magnetron sputtering technique. Figure 2 shows a schematic of DC magnetron sputtering system used in this study. Ionized argon (Ar+) particles bombard the Cr target assembled with a magnet. The energetic Cr atoms was deposited onto the rotating cladding surface with low rotation speed (~3 rpm). The technique secured densely packed layer growth without any porous structures. Depending on sputtering conditions,

surface morphology was modified [6]. Detailed sputtering condition can be found in Son et al.'s study [2].
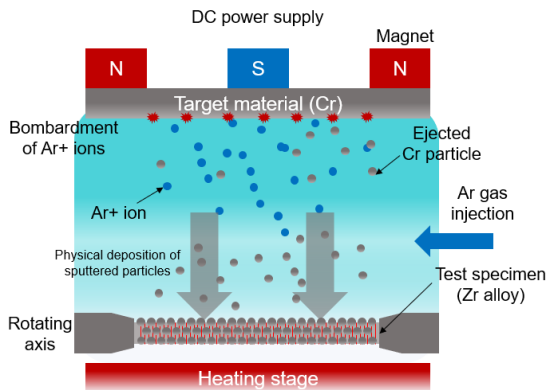
Fig. 2. Schematic of DC magnetron sputtering process.

2.3 Experimental conditions and procedure

For the preliminary experimental, a single reflooding flow condition was considered. The injection rate and subcooling of the coolant were 6.6 mm/s and 24°C, respectively at atmospheric pressure. Linear heat generation rate inside the test specimen was set to 2.23 kW/m, which is similar to the decay heat level during LOCA.

Experiments were carried out by following steps. First, the coolant was uniformly heated by circulation pump through the by-pass line. When the coolant reached the desired coolant subcooling condition (i.e. 24°C in this study), the DC power was applied through the copper electrodes. When the temperature measurement at location of z=60 mm reached about 780°C, the reflooding was initiated by using a three-way valve. The coolant injection and heat generation were continuously maintained until all the temperature recordings reached steady state. The boiling phenomena were visualized thorough a high-speed camera at frame rate of 500 fps. Temperature measurement data were saved at frequency of 10 Hz to capture the fast quench transition regime.

2.4 Data reduction

To evaluate the heat transfer performance, it is important to determine the surface heat flux. Because the TCs are located inside the test specimen under transient condition, it is challenging to evaluate the surface heat flux or temperature directly. Numerous previous studies [3-5] of pool type experiments utilized a lumped capacitance method, which considers the test specimen as a lumped volume. However, local boiling phenomena may vary along axial direction under reflooding condition. Thus, the lumped capacitance method could be applied in this study.

Instead, we carried out one-dimensional inverse heat conduction analysis by applying sequential function specification method suggested by Beck et al. [7]. It iteratively determines the surface temperature and heat flux that matches the measured temperature value. Specific algorithm can be found in Xiong et al.'s study [8].

3. Results and discussions

3.1 Temperature history

Figure 3 shows the temperature history measured from the TCs at z=20 and 60 mm. The history clearly showed the distinct boiling regimes appearing during the reflood. When the coolant level reached the TC position, the temperature started to decrease gradually indicating the film boiling regime. A dramatic temperature drop occurred when vapor film collapsed and boiling regime was in transit to nucleate boiling. In addition, it is noted that the temperature was still near 200°C despite that it reached steady state. Because continuous heat generation was maintained, the temperature was higher than the saturation temperature of the coolant.
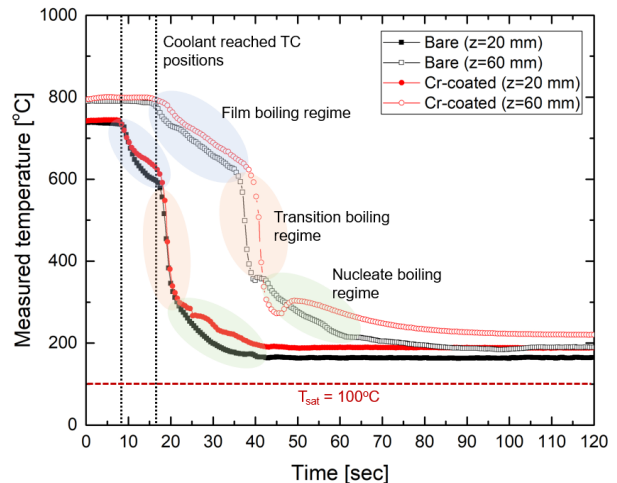
Fig. 3. Temperature history during the reflooding.

Overall the bare and Cr-coated specimen showed similar cooling performance. However, the Cr-coated surface showed an earlier collapse of film boiling regime at z=20 mm. This could be attributed to the enhanced wettability and increased surface area due to nanostructure of Cr-coated surface. According to the recent Son et al.'s study [2], the Cr-coated surface showed superhydrophilic characteristics with almost zero contact angle. In addition, Kwon et al. [9] noted that hierarchical micro/nanostructured surface resulted in a significant increase of MFBT (i.e. Leidenfrost temperature).

3.2 Boiling curve

Figure 4 shows the boiling curves of bare and Cr-coated specimens at z=20. The boiling curve shows the clear change of boiling regimes from film boiling to

nucleate boiling. The decreasing trend near the wall superheat of 600°C is result of inverse heat conduction analysis where initial radial temperature distribution of the specimen was assumed uniform with measured temperature. At z=20 mm, the Cr-coated surface showed the better cooling performance in terms of CHF and MFBT. The CHF of the Cr-coated surface (868 kW/m^2) was increased by 20% than that of bare surface (723 kW/m^2). The MFBTs of the bare and Cr-coated surfaces were 582°C and 626°C, respectively. Son et al. also reported 27% CHF enhancement of the surface with the same Cr-coating condition [2].
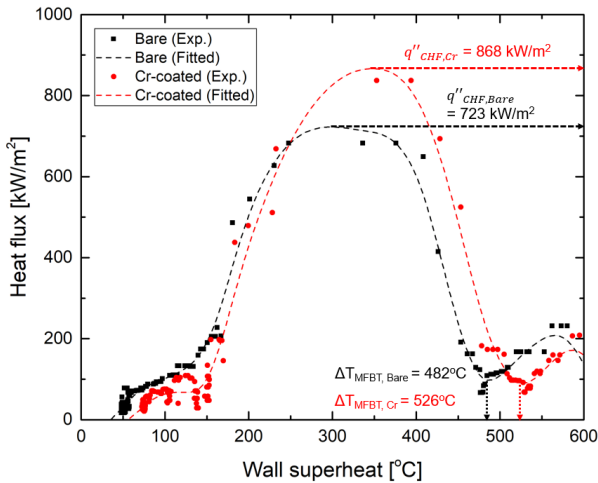
Fig. 4. Boiling curve of bare and Cr-coated surfaces at elevation of z=20 mm.

Figure 5 showed boiling curves of two surfaces at z=60 mm. Unlike the boiling curves at z=20 mm, the experimental data in nucleate boiling regime were widely scattered especially for Cr-coated surface. This is due to the sudden temperature increase at 40 and 45 sec for the bare and Cr-coated surfaces, respectively. Coalescence of rising bubbles generated from the bottom with the vapor film in elevated region hindered the efficient heat transfer by nucleate boiling. Thus, the increase of temperature during the cooling process induced some errors during the inverse conduction analysis. This phenomenon can be further explained by the high-speed visualization images in the next section.

In addition, it is important to note that the transition from film boiling to nucleate boiling occured at higher temperature than z=20 mm. The MFBTs of both surfaces were increased from 582°C to 617°C and 626°C to 634°C for bare and Cr-coated surfaces, respectively. It might not be deemed as a significant increase but considering that the local coolant subcooling decreased along the axial direction, it is worth noting that the MFBT was increased, which is opposite to general consensus [10]. As the surface was uniformly ground by the sandpaper, the surface parameter at each elevation should be equivalent. Thus, it is reasonable that the enhancement of MFBT at higher elevation was consequence of reflooding flow.
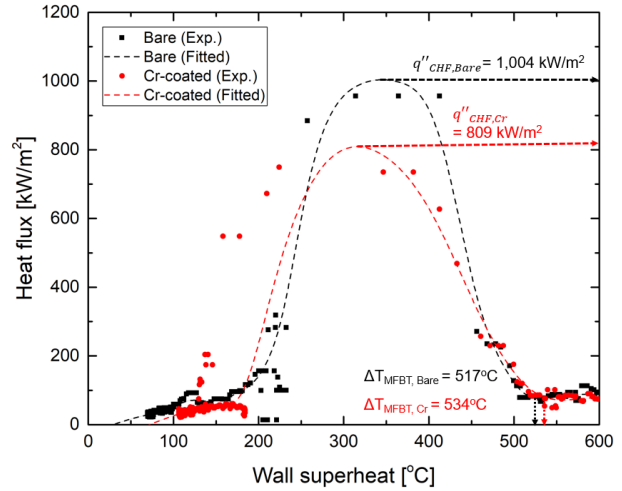
Fig. 5. Boiling curve of bare and Cr-coated surfaces at elevation of z=60 mm.

3.3 High-speed visualization

The reflooding flow effect on MFBT enhancement at upper region can be further analyzed through high-speed visualization images shown in Fig. 6. The images for the bare and Cr-coated surfaces were captured at equivalent time after the reflood. Quality difference of the images between the bare and Cr-coated surfaces was due to illumination technique. The red dashed lines indicate the position of the quench front where transition from film boiling to nucleate boiling takes place.
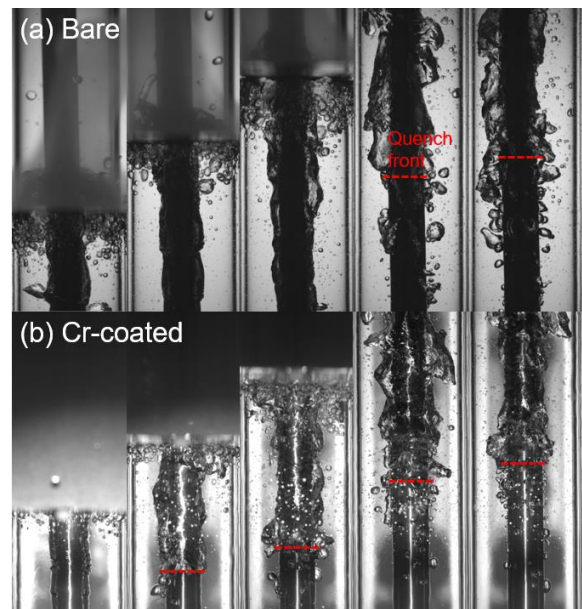
Fig. 6. High-speed visualization images during the reflood for (a) the bare and (b) Cr-coated surfaces.

It is noted that the quench front for the Cr-coated surface appeared much earlier than the bare surface. However, the quench front of the bare surface promptly propagated to the upper region as soon as it appeared from the bottom. In addition, it was observed that vapor

film at the beginning of the reflood was relatively stable in contrast to that of upper region. This is attributed to the nucleated bubbles generated from the bottom where the boiling regime already entered the nucleate boiling. The rising bubbles were coalesced with each other and escaped through the vapor film above. This resulted in an unstable and fluctuating vapor film. The bare surface showed the larger nucleated bubbles than the Cr-coated surface resulting in the larger fluctuation of vapor film. Superhydrophilic and nano-structured characteristics of the Cr-coated surface make bubbles smaller and difficult to be nucleated [2]. This coincides with the results in previous sections that the MFBT enhancement at z=60 mm was more significant for the bare surface.

3.4 Oxidation of specimens after the reflooding

As the purpose of Cr-coating is to mitigate the oxidation of the Zr-alloy cladding, the surface changes after reflooding were observed for the bare and Cr-coated surfaces. Figure 7 shows the pictures of the specimens before and after the reflood experiment. Clearly the bare surface was oxidized along the effective heated length showing darker color than original surface. On the other hand, the Cr-coated surface showed some green colored region at the center where temperature was the highest. This is attributed to the intrinsic green color of oxidized Cr particles (i.e. Cr_2O_3). It is reasonable to conclude that the Cr-coating layer was oxidized in place of Zr-alloy cladding. To properly evaluate the oxidation resistance of Cr-coated surface, further surface analysis by using the microscopy techniques are needed. In addition, the reason why the rainbow-like spectrum shown in Fig. 7(d) appeared is still unknown. It will be analyzed in the future works.
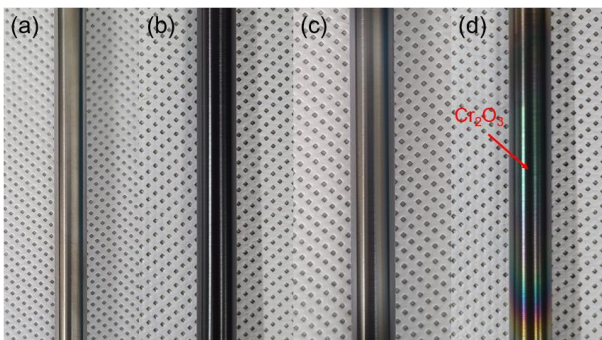
Fig. 7. Pictures of the bare and Cr-coated specimens before and after the reflood experiment: (a) Bare before the reflood, (b) Bare after the reflood, (c) Cr-coated before the reflood, and (d) Cr-coated after the reflood.

4. Conclusions

In this study, the heat transfer performance of Cr-coated Zr-alloy cladding during the reflood was investigated. Experiments were carried out with the specimen capable of simulating decay heat and with consideration of flow effect. Surface heat flux was obtained via the inverse heat conduction analysis. Results showed that Cr-coating resulted in enhancement of both CHF and MFBT due to increased wettability and capillary wicking. In addition, at higher elevation, higher MFBTs were observed due to vapor destabilization by nucleated bubbles generated at the lower part of the test specimen. Considering the fact that the surface parameters were equivalent and the coolant subcooling was decreased along the axial direction, the flow effect may play a significant role in determining the MFBT during the reflooding of the core. Additional experiments will be carried out as a future work to analyze the flow and surface modification effect.

REFERENCES

[1] Idaho National Laboratory, Investigations on the Thermal-hydraulic Behavior of Accident Tolerant Fuel Cladding Materials, INL EXT-19-56455, January, 2020.
[2] H. H. Son, Y. S. Cho, S. J. Kim, Experimental study of saturated pool boiling heat transfer with FeCrAl- and Cr-layered vertical tubes under atmospheric pressure, International Journal of Heat and Mass Transfer, Vol. 128, pp. 418-430, 2019.
[3] A. Seshadri, K. Shirvan, Quenching heat transfer analysis of accident tolerant coated fuel cladding, Nuclear Engineering and Design, Vol. 338, pp. 5-15, 2018.
[4] J. Y. Kang, T. K. Kim, G. C. Lee, M. H. Kim, H. S. Park, Quenching of candidate materials for accident tolerant fuel-cladding in LWRs, Annals of Nuclear Energy, Vol. 112, pp. 794-807, 2018.
[5] K. G. Lee, W. K. In, H. G. Kim, Quenching experiment on Cr-alloy-coated cladding for accident-tolerant fuel in water pool under low and high subcooling conditions, Nuclear Engineering and Design, Vol. 347, pp. 10-19, 2019.
[6] M. Nie, Growth and morphology evolution of semiconducting oxides and sulfides prepared by magnetron sputtering, Ph. D. thesis, Berlin, Germany, 2014.
[7] J. V. Beck, B. Blackwell, C. Clair, Inverse heat conduction: Ill-posed problems, John Wiley & Sons, Inc., 1985.
[8] J Xiong, Z. Wang, P. Xiong, T. Lu, Y. Yang, Experimental investigation on transient boiling heat transfer during quenching of fuel cladding surfaces, International Journal of Heat and Mass Transfer, Vol. 148, 119131, 2020.
[9] H. M. Kwon, J. C. Bird, K. K. Varanasi, Increasing Leidenfrost point using micro-nano hierarchical surface structures, Applied Physics Letters, Vol. 103, 201601, 2013.
[10] S. A. Ebrahim, S. Chang, F. B. Cheung, S. M. Bajorek, Parametric investigation of film boiling heat transfer on the quenching of vertical rods in water pool, Applied Thermal Engineering, Vol. 140, pp. 139-146, 2018.